8

# Integrated numerical procedures for the design, analysis and optimization of diesel engines

Daniela Siano[1], Fabio Bozza[2] and Michela Costa[1]
[1]*Istituto Motori – CNR*
[2]*DIME – Università di Napoli*
*ITALY*

## 1. Introduction

Both the design and analysis of a diesel engine requires the integration of accurate theoretical methods, resorting to 1D - 3D CFD modelling and vibro-acoustic engine analysis. In this chapter, the above numerical approaches will be deeply presented and integrated to perform a diesel engine design and/or analysis. As known in fact, the possibility to simulate the physical and chemical processes characterising the operation of internal combustion engines by using appropriate codes and high performance computers is continuously spreading. These simulations can predict, as an example, fuel consumption, toxic emissions and noise radiation. By varying the design and/or control parameters, different engine configurations or working conditions can be tested and their performances compared. Optimization techniques (Papalambros et al. 2000; Stephenson, 2008; Costa et al., 2009), properly matched with the various simulation procedures, are hence the most suitable tool to identify optimal solutions able to gain prescribed objectives on engine efficiency, power output, noise, gas emissions, etc.. The choice of the optimization goal, moreover, strictly depends on the application type and the definition of a compromise solution among the conflicting needs is in many cases required.
Concerning the design of a combustion engine, a complicated and multi-objective task is to be afforded, since it generally requires the fulfilment of various objectives and constraints, as high efficiency and power output, low noise and gas emissions, low cost, high reliability, etc. A tool for multi-objective optimization, therefore, can be considered as fundamental at the engine design stage, in order to gain insight into the complicated relationships between the physical entities involved in the design and design-dependent parameters. Ultimately, optimization can greatly reduce the time-to-market of new engine prototypes.
Optimization techniques can successfully be applied to analyze the operating conditions of existing engines, too. In this case, the optimization process can be focused on the selection of the control parameters in order to obtain an optimal engine behaviour. It is well known, in fact, that combustion development and emission production depend on a complex interaction among different parameters, namely injection modulation and phasing (Stotz et al. 2000), boost pressure, EGR fraction, swirl ratio, fuel properties, and so on. The optimal choice of a so large number of parameters depends on speed and load conditions, and it is

related to the fulfilment of a number of contrasting objectives, like reduced NOx, Soot, HC, CO, fuel consumption and noise emissions.
In the present chapter the cited approach to the design and analysis of a diesel engine will be explained. The discussion will be organized in the following paragraphs, each regarding a different case study. In particular, the first paragraph is focused on the description of single methodologies and to their integration:

- A 1D simulation of the whole propulsion system is realized by means of a proprietary code. It allows to determine engine-turbocharger matching conditions and is able to compute pressure, temperature and gas composition at the intake valve closure. The latter data represent initial conditions for the successive 3D analysis.
- A 3D simulation of the engine cylinder is developed by exploiting geometrical information derived by the engine CADs. The in-cylinder pressure cycle during the closed valve period, is predicted, starting from the initial conditions provided by the 1D code.
- 1D or 3D computed pressure cycles are then utilized within vibro-acoustic analyses aiming to estimate the combustion radiated noise. Depending on the application, different approaches are followed:
    - FEM-BEM approach: FEM analysis is applied to determine the vibration of the engine skin surface; Direct Boundary Element Method (DBEM) solves the exterior acoustic radiation according to the ISO directives, to predict the radiated overall noise level. This method is utilised during the engine design phase.
    - Simplified approach: An analytical model based on the decomposition of in-cylinder pressure cycles is developed to estimate the radiated noise level. Some coefficients included in the above correlation are properly tuned to get a good agreement with the acoustic experimental data. This method is applied during the engine analysis phase.
- The numerical models are in different ways coupled to the optimization code, to identify the optimal design parameters or the injection strategies, to the aim of realizing the maximization of the engine performance, the reduction of the NOx and soot emissions, and the reduction of the radiated noise, at a constant load and rotational speed.

The second paragraph illustrates the design and optimization of a new two-stroke diesel engine suitable for aeronautical applications. The engine, equipped with a Common Rail fuel injection system, is conceived in a two-stroke uniflow configuration, aimed at achieving a weight to power ratio equal to one kg/kW. Both CFD 1D and 3D analyses are carried out to support the design phase and to address some particular aspects of the engine operation, like the scavenging process, the engine-turbocharger matching, the fuel injection and the combustion process. The exchange of information between the two codes allows to improve the accuracy of the results. Computed pressure cycles are also utilized to numerically predict the combustion noise, basing on the integration of FEM and BEM codes. The obtained results are suitable to be used as driving parameters for successive engine optimization. In order to improve the engine performance and vibro-acoustic behaviour, the

1D model, tuned with information derived from the 3D code, is linked to the optimization code. A constrained multi-objective optimization is performed to contemporary minimize the fuel consumption and the maximum in-cylinder temperature and pressure gradient directly related to the noise emission. In this way a better selection of a number of engine parameters is carried out (exhaust valve opening, closing and lift, intake ports heights, start of injection, etc).

The third paragraph, indeed, describes an environmental and energetic optimization of a naturally aspirated, light-duty direct injection (DI) diesel engine, equipped with a Common Rail injection system. An experimental campaign is initially carried out to gain information on performance and noise levels on the engine and to acquire the data required to validate the 1D, the 3D model and the combustion noise procedure. As in the previous case, a preliminary numerical simulation is carried out. Then, an optimization process is settled in order to identify the control parameters of a three pulses injection profile, for a constant overall mass of injected fuel. These parameters are assumed as independent variables of the multi-objective optimization tool and are selected with the aim of simultaneously minimizing fuel consumption, pollutant emissions and radiated noise.

## 2. Numerical Procedures

**1D Simulation**: the 1D simulation of the whole propulsion system is realized by means of the 1Dime software developed at the Mechanical Engineering Department of the University of Naples "Federico II" (Siano et al., 2008, Costa et al., 2009) and by exploiting geometrical information of the intake and exhaust system derived by the engine CAD. The whole engine is firstly schematized as a network of pipe and plenums, then, the 1D flow equations are solved in each pipe constituting the intake and the exhaust system. The gas inside the cylinder is indeed treated as a zero-dimensional thermodynamic system.
The code solves the 1D flow equations in the intake and exhaust pipes:

$$\mathbf{U}=\begin{Bmatrix}\rho\\ \rho u\\ \rho E\\ \rho x_r\\ \rho x_f\end{Bmatrix}\quad \mathbf{F}=\begin{Bmatrix}\rho u\\ \rho u^2+p\\ \rho u H\\ \rho u x_r\\ \rho u x_f\end{Bmatrix}\quad \mathbf{S}=-\begin{Bmatrix}\rho u\dfrac{1}{\Omega}\dfrac{d\Omega}{dx}\\ \rho u^2\left[\dfrac{1}{\Omega}\dfrac{d\Omega}{dx}+\left(2\dfrac{f}{D}+\dfrac{C_p}{2L}\right)\dfrac{u}{|u|}\right]\\ \rho u H\dfrac{1}{\Omega}\dfrac{d\Omega}{dx}-4\dfrac{q}{D}\\ \rho u x_r\dfrac{1}{\Omega}\dfrac{d\Omega}{dx}\\ \rho u x_f\dfrac{1}{\Omega}\dfrac{d\Omega}{dx}\end{Bmatrix} \tag{1}$$

where ρ, u, p, $E=c_vT+u^2/2$, $H=c_pT+u^2/2$ respectively represent the density, the velocity, the pressure, and the total energy and enthalpy per unit mass. The source term **S** takes into account the duct area variation along the flow direction, dΩ/dx, the wall heat exchange, q,

and the friction losses. The last two equations describe the scalar transport of chemical species, $x_r$ and $x_f$ being the residual gases and fuel mass fraction, respectively. These equations allow to compute the composition of the gases flowing in the intake and exhaust systems and therefore to estimate also the in-cylinder charge composition.
In the case of turbocharged engine, the performance maps of the turbocharger group are employed to compute the engine-turbocharger matching.
Concerning the modeling of the combustion process, a classical Wiebe equation is utilized to compute the heat release rate in the engine. Proper values of the combustion process duration during both premixed and diffusive phases are specified. This preliminary approach is substituted in the following by the more detailed 3D analysis later described.

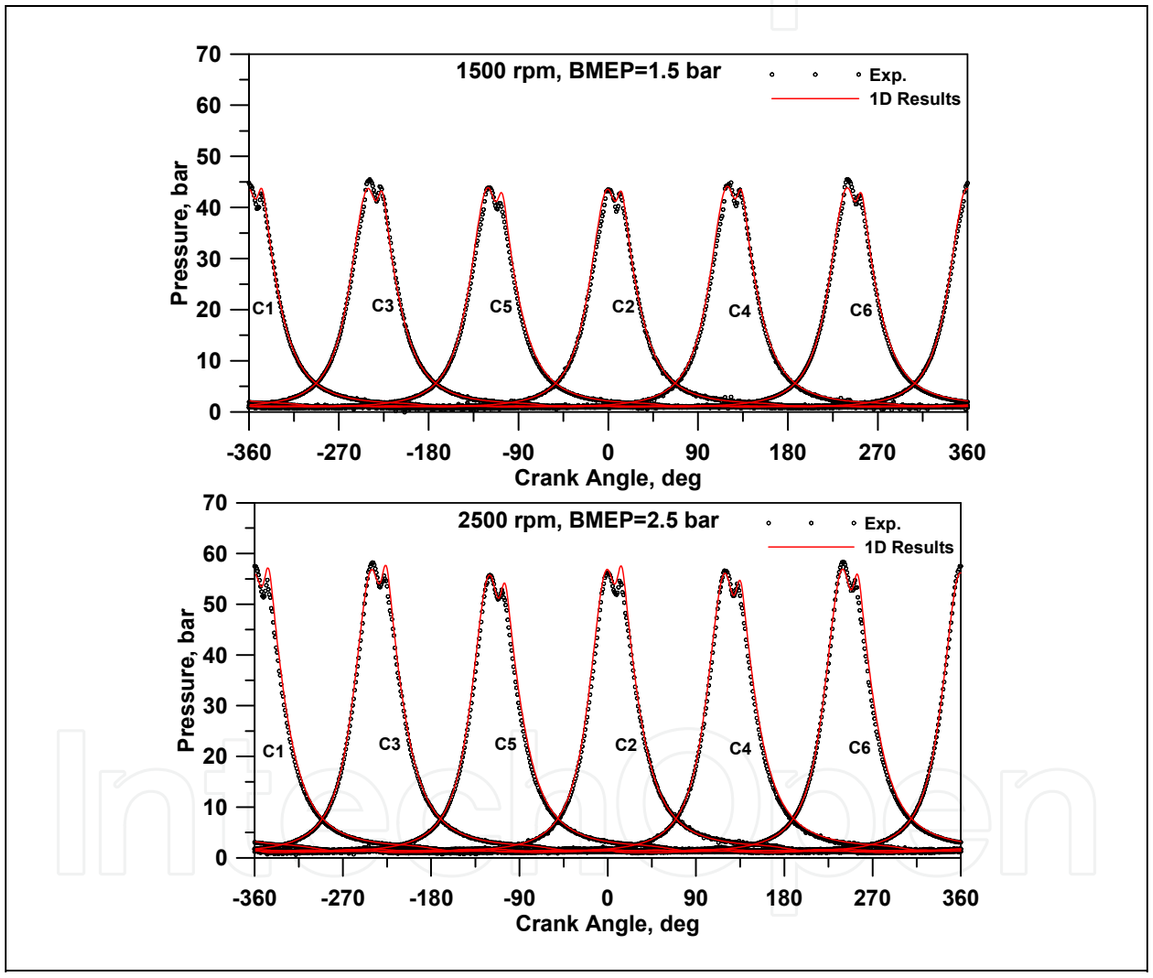


Fig. 1. 1D computed pressure cycles in different operating conditions

As an example, Figure 1 displays the comparison between computed and experimental pressure cycles in a turbocharged six cylinders engine, for two different operating conditions. The agreement along the compression stroke indicates that a good engine-turbocharger matching can be reached. Starting from the computed initial conditions at IVC, the 3D model is expected to further improve combustion phase analysis.

**3D Simulation**: The AVL FIRE™ 3D code is employed. It represents a multipurpose tool, specially conceived for engine applications. The first step of the analysis concerns the generation of the 3D domain representing the computational grid. This is effected by means of the semi-automatic procedure of the code, named Fame Advanced Hybrid, which allows to reach a good compromise between accuracy and reduced number of cells. The computational period is subdivided into intervals, each pertinent to a grid of a chosen size, that is deformed as the piston moves until predefined crank angles, starting from which new grids with different sizes are used. This occurs through a procedure of re-mapping of the computed variables, termed rezone, avoiding an excessive cells deformation. Within each cell, the Reynolds Averaged Navier-Stokes equations are numerically solved to compute the 3D flow field and the thermodynamic conditions inside the cylinder. The CFD analysis accounts for the fuel spray dynamics and for the subsequent chemical reactions, leading to the prediction of the rate of heat release (Colin and Benkenida, 2004) , pollutants formation and in-cylinder pressure cycle.
The fuel spray spatio-temporal dynamics is simulated according to a Discrete Droplets Model (DDM) (Liu and Reitz, 1993; O'Rourke. 1989; Dukowicz, 1980), where the Eulerian description of the gaseous phase is coupled with a Lagrangian approach to the study of the liquid flow. Modelling of spray accounts for primary and secondary atomization, evaporation, coalescence, turbulence effects and possible cavitation within the nozzle. Examples of spray, combustion and emission calculations will be presented in paragraphs 2 and 3, with reference to selected case studies.

Despite the modelling of the combustion and noxious emission, the 3D code can be also employed to improve the accuracy of the previously described 1D model through the theoretical evaluation of the discharge coefficients through valves or ports. The above values are usually derived from literature information in 1D modelling and, of course, the related accuracy is limited. Alternatively, the latter can be evaluated by numerically simulating the 3D air flow within the engine intake system. The computation is performed under the hypothesis of steady conditions, in such a way to reproduce a possible experiment realisable over a flow rate test bench. An example grid used for this kind of analysis is shown in Figure 2. It refer to a two-stroke engine more deeply described in paragraph 2 and clearly exhibits the geometrical characteristics of the air admission volume, with one inflow duct and the three cylinders of a bank placed with their axes in the direction orthogonal to that of the air inflow. Only the central cylinder is considered as opened. The volume corresponding to the intake ports of the central cylinder is meshed, those of the lateral cylinders are not included in the computational domain for the sake of simplicity. The total number of cells is 518346, 330746 of which are hexahedrical, thus assuring a certain grid regularity. The fourteen ports of the central cylinder form one block with an external cylindrical area, whose design follows the geometric characteristics of the cylinder jacket. The grid in this zone, quite well visible in Figure 2, is made particularly thick, since it comprehends 148415 cells. Computation is performed for fixed values of the entering air mass flow rate and always setting the static pressure and temperature at the outlet section equal to atmospheric conditions. The ports are opened to the 100%, 75%, 50% and 25% for a mass flow rate ranging from 0.03 to 0.15 kg/s.
Figure 3 shows a view of the velocity magnitude distribution obtained as a result of the calculation for intake ports completely opened. The velocity vector magnitude is considered

over a plane orthogonal to the cylinders axes, cutting the intake ports exit section in the middle. Air velocity distributes non-uniformly over the fourteen ports surfaces: the seven ports which are closer to the air inflow duct are better served and mainly contribute to fill the cylinder with the fresh charge. The velocity in correspondence of the other seven ports maintains lower. The shape of the ports, with their surfaces positioned in tangential direction with respect to the cylinder external surface, allows a swirl motion of the air entering the cylinder.

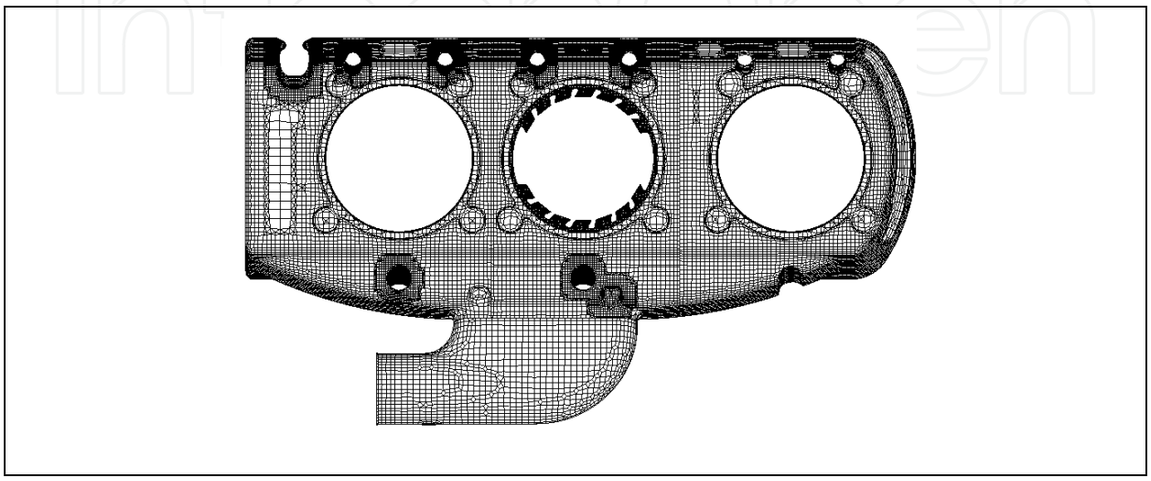

Fig. 2. Grid employed for the evaluation of the intake ports discharge coefficient.

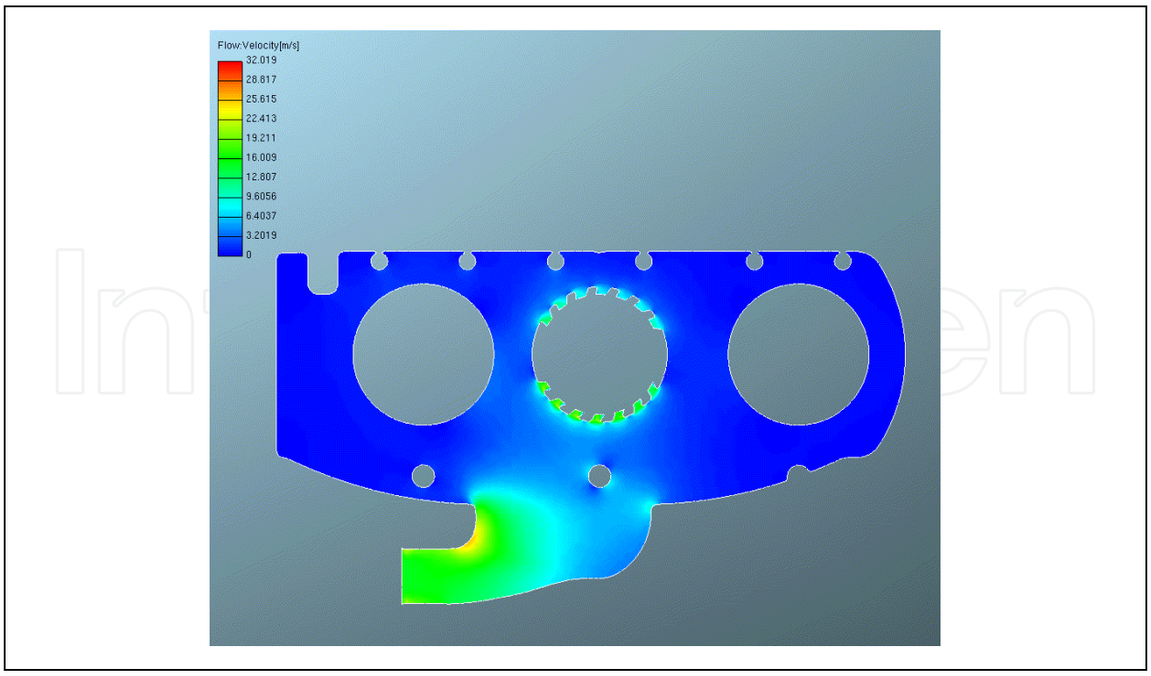


Fig. 3. Velocity field on a plane orthogonal to the cylinder axis

The results of the computations allow the determination of the discharge coefficient as the ratio between the effective mass flow rate, $\dot{m}_{eff}$ , and the theoretical one, $\dot{m}_{th}$ :

$$C_D = \frac{\dot{m}_{eff}}{\dot{m}_{th}} \tag{2}$$

The theoretical mass flow rate is evaluated as a function of inlet pressure and temperature and flow area, corresponding to the imposed effective mass flow rate.
Figure 4 summarises the results of the calculation for various surface percentages in the opening of the intake ports. The discharge coefficient maintains almost constant with the entering mass flow rate and ranges between about 0.6 and 0.98, due to the reduction of the exit section area used for the evaluation of the theoretical mass flow rate. These results will be directly employed in the 1D model, for accuracy improvement.

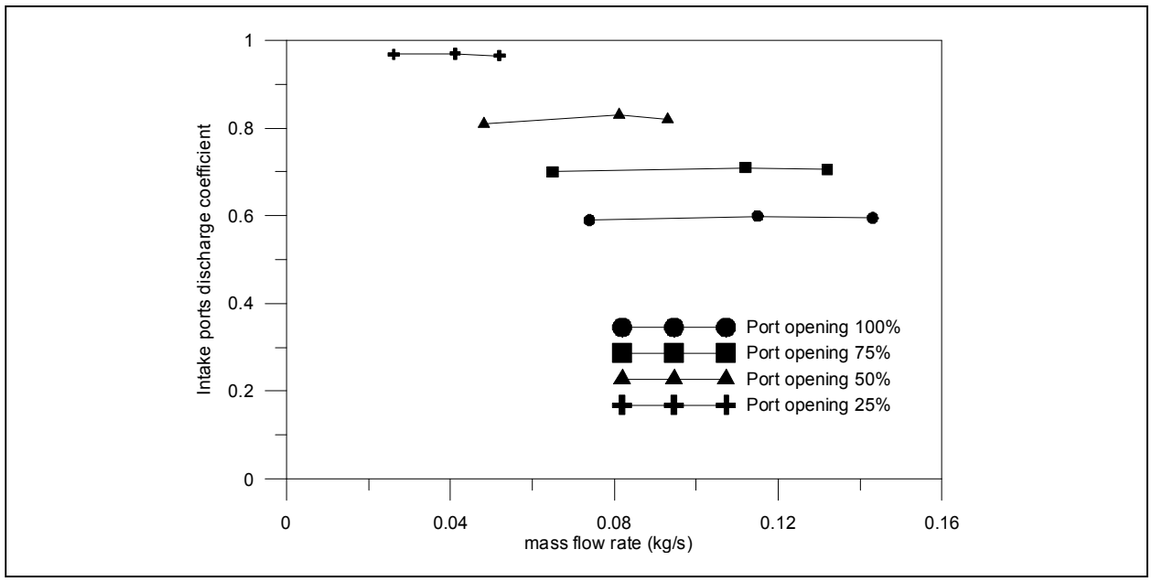


Fig. 4. Discharge coefficients evaluated for various opening of the intake ports.

**Vibro-acoustic analyses**: a FEM analysis is conducted in order to evaluate the engine surface vibrations induced by the combustion process evolution. The previously predicted pressure cycle is employed in this phase to compute the forces acting on the internal structure. The obtained vibrational output data represent the boundary conditions to be applied to the BEM code for the final evaluation of the radiated sound power. The selected codes to evaluate the sound radiation noise from the engine block surface are the MSC/Nastran™ and LMS/Sysnoise™. Both approaches require the development of a detailed 3D mesh and are very time-consuming. For this reason, this detailed methodology cannot be directly applied within the optimization loop. Additional insights of the above summarized approach will be given in paragraph 2.

Alternatively, a simplified and recently proposed methodology (Torregrosa et al., 2007; Payri et al., 2005) can be utilized for the prediction of the overall combustion noise, which

includes in the correlation a strict dependency on the engine operating conditions and injection strategy. The main idea behind this technique is the decomposition of the total in-cylinder pressure signal according to three main contributions: compression-expansion, combustion and resonance pressures:

$$p_{tot} = p_{mot} + p_{comb} + p_{res} \tag{3}$$

The first contribution (also referred as pseudo-motored signal) is only related to volume variation, and is used as a reference signal. It is determined by a direct in-cylinder pressure acquisition during a fuel switch-off operation. The third term (resonance pressure) is indeed related to high-frequency pressure fluctuations, induced by the wave reflections in the combustion chamber, mainly occurring at autoignition time. It is computed through a high pass-band filter (above 4500 Hz) of the total pressure signal. By difference, the combustion pressure (second term in eq. 3) can be easily determined, too. The three terms in eq. 3 are reported for comparison in figure 5. Despite the presence of the previously discussed high-frequency amplitudes, the resonant pressure is significantly lower than other contributions. Nevertheless, it may still exert a non-negligible effect on the overall noise.

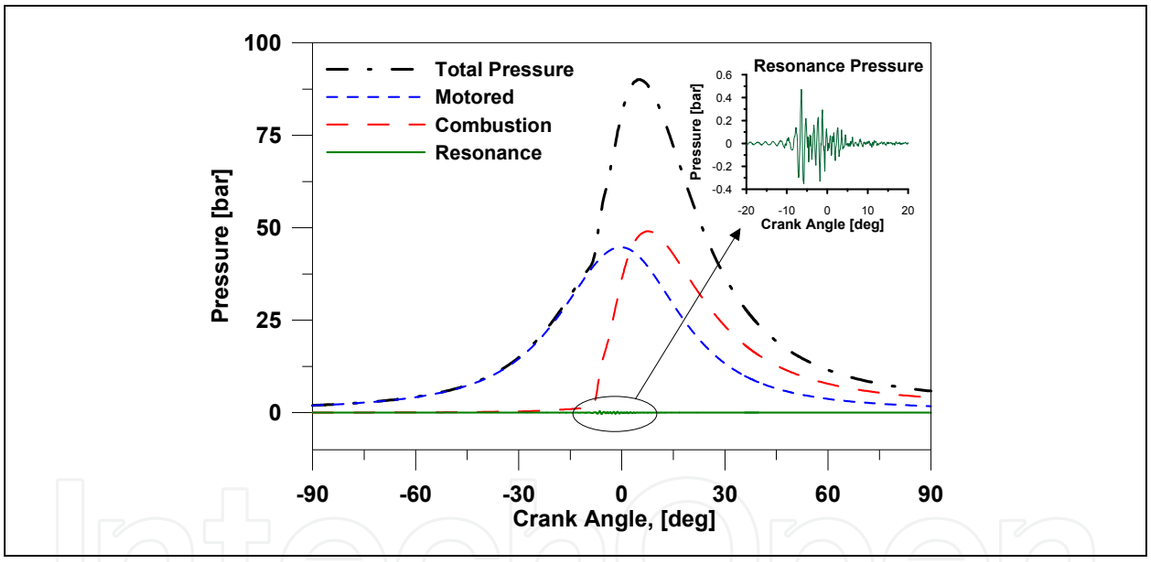


Fig. 5. Decomposition of the total pressure in motored, combustion and resonance contributions.

The three decomposed pressures are utilized to compute two characteristic indices $I_1$ and $I_2$ defined as:

$$I_1 = \frac{n}{n_{idle}} \left[ \frac{\left( \frac{dp_{\max 1}}{dt} \right)_{comb} + \left( \frac{dp_{\max 2}}{dt} \right)_{comb}}{\left( \frac{dp_{\max}}{dt} \right)_{mot}} \right] \tag{4}$$

$$I_2 = \log_{10}\left[10^6\left(\frac{\int p_{res}^2 dt}{\int p_{mot}^2 dt}\right)\right] \tag{5}$$

The $I_1$ index is a function of the maximum pressure gradient of the combustion contribution, occurring after the pilot $(dp_{max1}/dt)c_{omb}$ and the main injection $(dp_{max2}/dt)_{comb}$. The $I_1$ index is also non-dimensionalized over the maximum pressure gradient of the pseudo-motored pressure $(dp_{max}/dt)_{mot}$. In the case of a single-shot injection, a unique term is of course present in the eq. (4) numerator. The $I_2$ index takes into account the acoustic energies ($\int p^2 dt$) associated with resonance and motored pressure signals. An additional index In is finally defined accounting for mechanical noise contribution, related, as stated, to the sole engine speed:

$$I_n = \log_{10}\left(\frac{n}{n_{idle}}\right) \tag{6}$$

n being the engine speed and $n_{idle}$ the idle rotational speed.
Basing on the above definitions, the Overall Noise (ON) can be finally computed as:

$$ON = C_0 + C_n \cdot I_n + C_1 \cdot I_1 + C_2 \cdot I_2 \tag{7}$$

$C_i$ being proper tuning constants, depending on the engine architecture and size.
Following the relations (4-7), a Matlab routine was developed to properly process the in-cylinder pressure cycle and compute the various noise indices and the overall noise.
The method is validated on acoustic measurements taken on a commercial engine, as reported in figure 6. The agreement obtained is satisfactory at each engine speed. A maximum absolute error of about 1.3 dB is found at a medium engine regime.

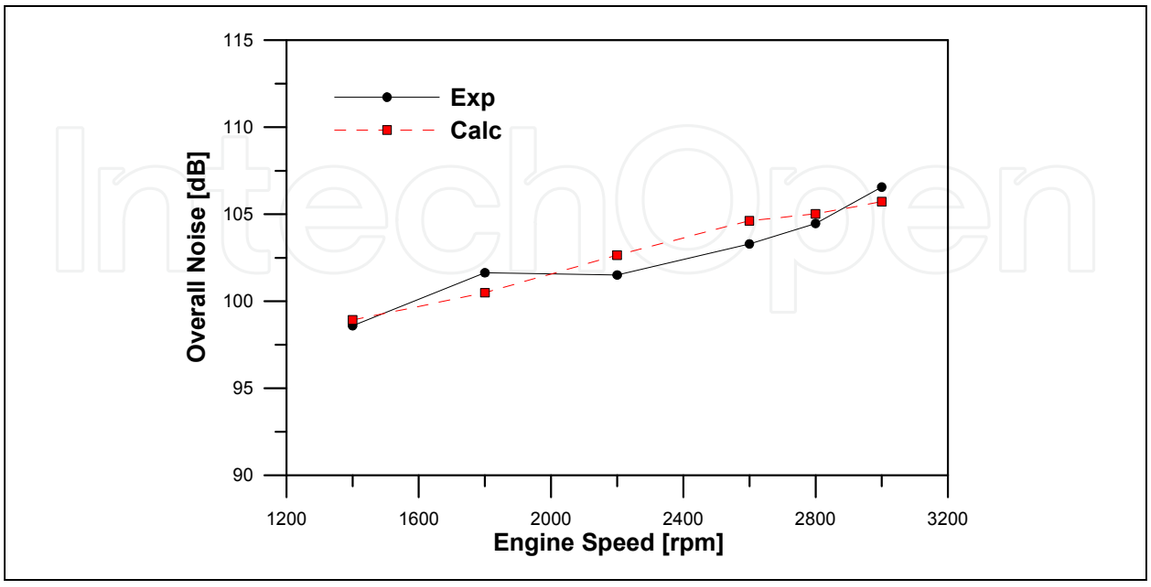


Fig. 6. Comparisons on the overall noise

The method can be applied to both experimental and numerical pressure cycles and strictly depends on the engine operating conditions and injection strategy. Once validated, this simplified approach is directly included in the optimization loop to predict the overall noise.

**Optimization process**: the briefly described 1D, 3D and acoustic tools are coupled together within an optimization loop searching for design or control parameters minimizing fuel consumption, gaseous emissions and radiated noise. The logical development of the optimization problem is developed within the ModeFRONTIER™ environment. For each set of the design or control parameters, the 1D, 3D and acoustic tools are automatically started. 1D results allow to run the 3D code from reliable conditions at the intake valve closure. Then, the 3D computed pressure cycle is automatically given in input to a Matlab™ routine computing the overall combustion noise. Simultaneously, the Indicated Mean effective pressure (IMEP), is returned back to the optimizer, together with the NO and soot levels at the end of the 3D run. A multi-objective optimization is so defined to contemporarily search the maximum IMEP, the minimum soot, the minimum NO and the minimum overall noise. To solve the above problem, genetic algorithms (Sasaki, 2005) are usually utilized, employing a range adaptation technique to overcome time-consuming evaluations. As usual in multi-objective optimization problems, a multiplicity of solutions is expected, belonging to the so-called Pareto frontiers. In order to select a single optimal solution among the Pareto-frontier ones, the "Multi Criteria Decision Making" tool (MCDM) provided in modeFRONTIER™ is employed. This allows the definition of preferences expressed by the user through direct specification of attributes of importance (weights) among the various objectives. Depending on these relations, the MCDM tool is able to classify all the solutions with a rank value. The highest rank solution is the one that better satisfies the preference set.

In the following paragraphs, two examples are presented where the described methodology is applied to perform the design of a Two-Stroke Engine for aeronautical application and to select an optimal fuel injection strategy for a light-duty automotive engine.

## 3. Optimal Design of a Two-Stroke Engine for aeronautical application

In this paragraph, some aspects concerning the development of a prototype of a diesel engine suitable for aeronautical applications are discussed (Siano et al., 2008). The engine aimed at achieving a weight to power ratio equal to one kg/kW (220 kg for 220 kW) is conceived in a two stroke Uniflow configuration and is constituted by six cylinders distributed on two parallel banks. Basing on a first choice of some geometrical and operational data, a preliminary fluid-dynamic and acoustic analysis is carried out at the sea level. This includes the engine-turbocharger matching, the estimation of the scavenging process efficiency, and the simulation of the spray and combustion process, arising from a Common Rail injection system. Both 1D and 3D CFD models are employed.
A CAD of the engine under investigation is shown in figure 7. Six cylinders are distributed on two parallel banks with separate air admission. The supercharging system consists of a dynamical turbocharger coupled to a mechanical one (of the roots type), serving the engine start-up, as well. An automotive derived roots compressor is chosen with a transmission-ratio equal to 5. As a first step, a preliminary 1D simulation of the entire propulsion system

is realized by means of the previously described 1D software, and by exploiting geometrical information derived by the engine CAD. Figure 8 reports the engine 1D schematization including the three cylinders, the turbocharger group (C-T), the intercooler (IC) and the mechanical supercharger (C), coupled to the engine shaft. A waste-gate valve (BY) is also considered upstream of the turbine. Half engine is schematized, due to the symmetry property of the two engine banks. Each of the three cylinders is connected to the intake plenum through fourteen inlet ports and to the exhaust plenum through two exhaust valves. In the 1D computation, the 3D computed discharge coefficients are employed. Scavenging is indeed considered as in the middle between the two opposite limits so-called of perfect displacement and perfect mixing. In other words, a parameter, wmix, representing a relative weight factor between the occurrence of a perfect mixing and a perfect displacement process, is assumed equal to the value of 0.67. The above parameter results, once again, from accurate analyses carried out on the engine cylinder by means of the 3D code (figure 9).

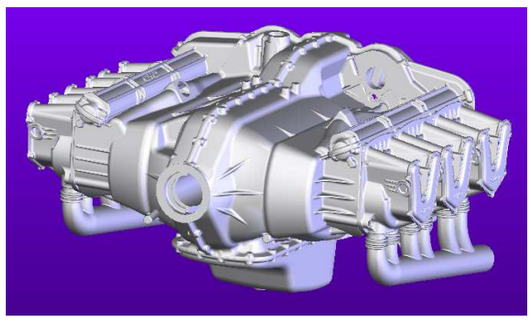

Fig. 7. 3D cad view of the 6 cylinder, two-stroke Diesel engine.

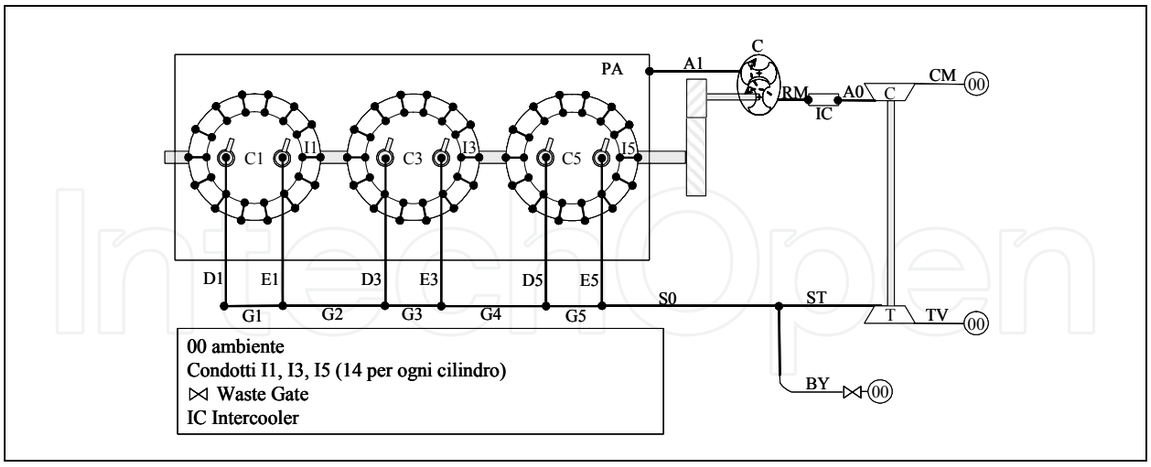


Fig. 8. 1D schematization of the AVIO3 engine

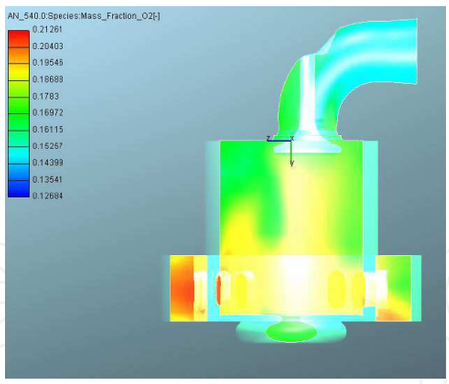


Fig. 9. 3D analysis for the calculation of the scavenging efficiency

The 3D analysis also provides the definition of a proper heat release law, to be included in the 1D model, assuming injection in one shot. Figure 10 shows the 3D computed pressure cycle in comparison with the results of the 1D model. An idea of how the injection strategy affects combustion is also given. It is evident that a too advanced injection makes for a too much high pressure peak, which may be dangerous in terms of mechanical stresses, whereas a late injection makes for a low cycle area, hence a low power output and high fuel consumption.

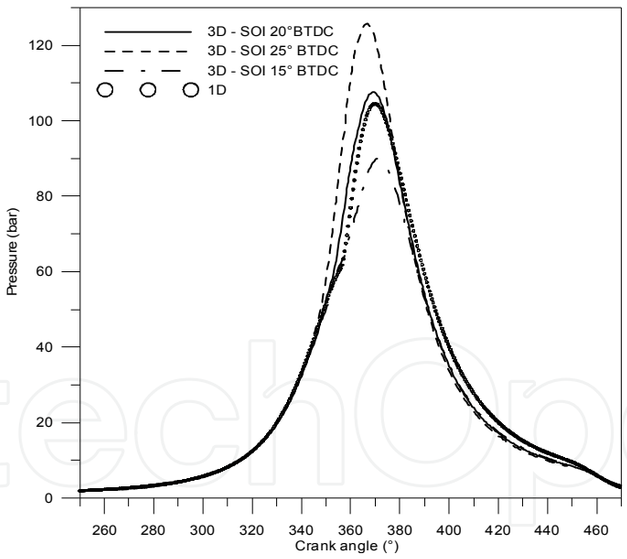


Fig. 10. Comparison of the in-cylinder pressure as obtained by the 1D and the 3D codes for SOI at 20° BTDC. The 3D simulations are also relevant to SOI at 15° and 25° BTDC.

In parallel to the 1D and 3D analyses, an acoustic study is also carried out to predict the combustion noise
radiation following the FEM/BEM approach.

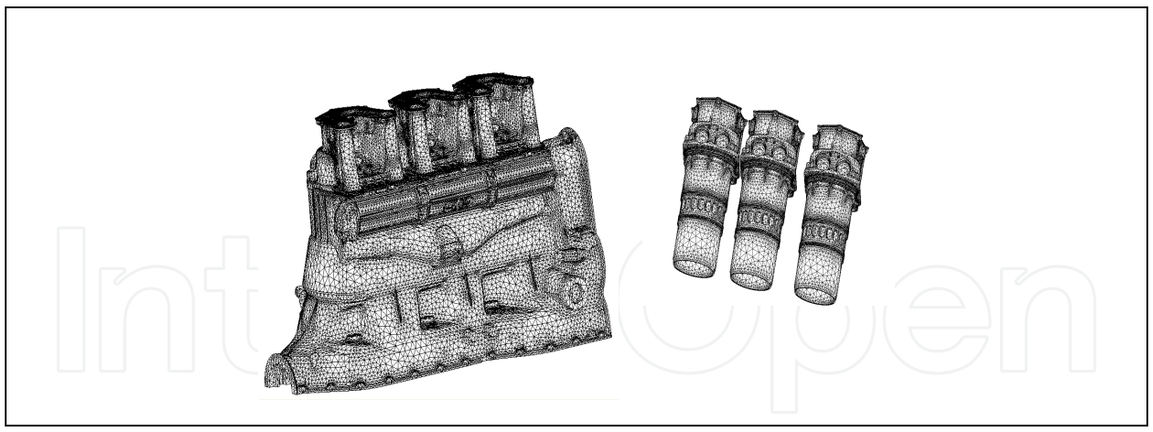

Fig. 11. Mesh models of the engine block and cylinder liners.

In particular, the FE model is developed subdividing the engine into single groups, each manually meshed and finally assembled. Two parts are mainly considered, as shown in Figure 11: the engine block and the cylinder liners. A non automatic meshing process is required to handle the great complexity of the cylinder geometry especially concerning the presence of the fourteen inlet ports. With the purpose of getting information about the skin surface vibrations, a frequency response analysis is conducted using as excitation the 1D computed pressure forces acting inside the cylinders during the combustion process at the 2400 rpm engine speed.

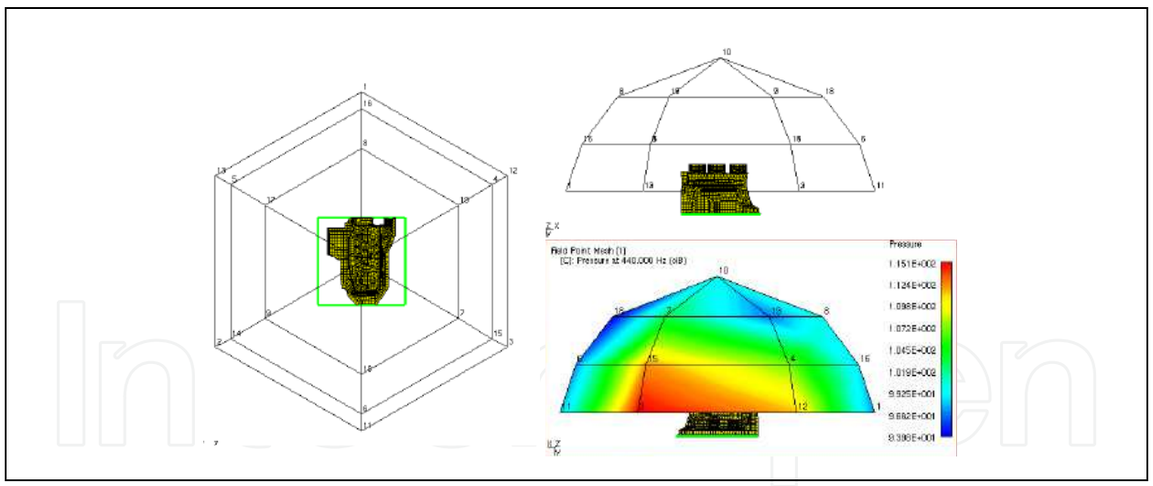

Fig. 12. Hemispherical surface with field points and Sound Power map according to the ISO 3746 directive.

Beside the calculation of the surface velocity, a boundary element mesh is realised with a reduced number of nodes and elements. The obtained vibrational output data represent the boundary conditions to be applied to the BEM for the final evaluation of the radiated sound power. The approach used is the ATV methodology (Acoustic Transfer Vectors). This technique, through the preliminary evaluation of the transfer functions of surface-receivers (microphones), allows to evaluate the answer to different boundary conditions, as the

application of fine-loads or multi-frequency excitations (engine noise). The acoustic radiation can be so evaluated from the calculation of the sound pressure on a virtual measurement surface that completely contains the radiant surface.
For the measurement of the radiated power, an hemispherical surface is created around the engine model, according to normative ISO 3746.
Figure 12 shows the above surface, positioned at the distance of one meter from the engine, which includes the nineteen field points (virtual microphones) used to get information about the noise radiation. In the same figure the resulting sound pressure map is also plotted. In particular, it is possible to note that the major contribution to the overall noise comes from a lateral part, corresponding to the carter, which presents a smaller thickness with respect to the other engine parts. A non negligible contribution also comes from the engine top, excited by the subsequent combustion process events.
Figure 13 displays the frequency spectrum of the average sound power radiation on the surface. It is important to remark the presence of two tonal peaks at the frequencies of 440 Hz (118 dB) and 1060 Hz corresponding to a resonance phenomenon with the fundamental firing frequency at about 40 Hz (2400 rpm).
In conclusion, it can be stated that a great noise radiation is revealed in correspondence of resonance conditions.
This kind of integration of different numerical procedures allows to predict, with a good accuracy, the engine radiated noise and can be used in a pre-design phase in order to characterize the acoustic behaviour of the engine structure.

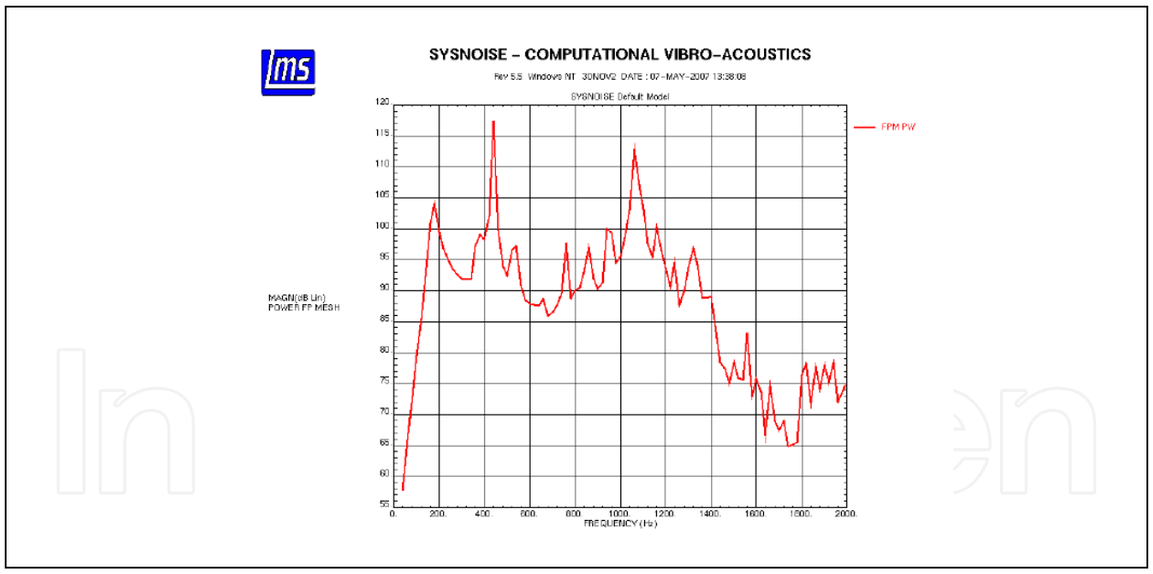


Fig. 13. Average Sound Power radiation on the hemispherical surface.

The iterative exchange of information between the 1D and 3D codes allows to define the main performance outputs of the engine under development. Although the numerical analysis confirms the possibility to reach the prescribed power output with the imposed limitation on the maximum pressure (126 bar), it also puts into evidence the occurrence of a high value of the Brake Specific Fuel Consumption (BSFC = 258 g/kWh). The acoustic analysis also estimates the presence of a high combustion noise level, with a sound power

peak of about 118 dB, strictly related, as known, to the maximum in-cylinder pressure gradient reached during the combustion process.

In order to improve the overall performance characteristics of the engine, an optimization procedure is carried out to the aim of finding a better selection of some geometrical and operating parameters. In particular, a different phasing of both exhaust valves and intake ports is considered, together with a different phasing of the injection law. The above parameters actually affect also the supercharging level, and, for this reason, the 1D code must be mandatory utilized in the optimization procedure. The 1D analysis, however, includes the details of the previous 3D study in terms of both scavenging efficiency, discharge coefficients and heat release rate.
Figure 14 displays the logic chart of the optimization procedure, developed in the ModeFrontier graphical environment. The independent variables considered are:

- EVO: Exhaust Valve Opening, deg
- EVD: Exhaust Valve Duration, deg
- EVL: Exhaust Valve Lift, mm
- IPO: Intake Port Opening, deg
- IPL: Intake Port width, mm
- THJ: Start of injection, deg

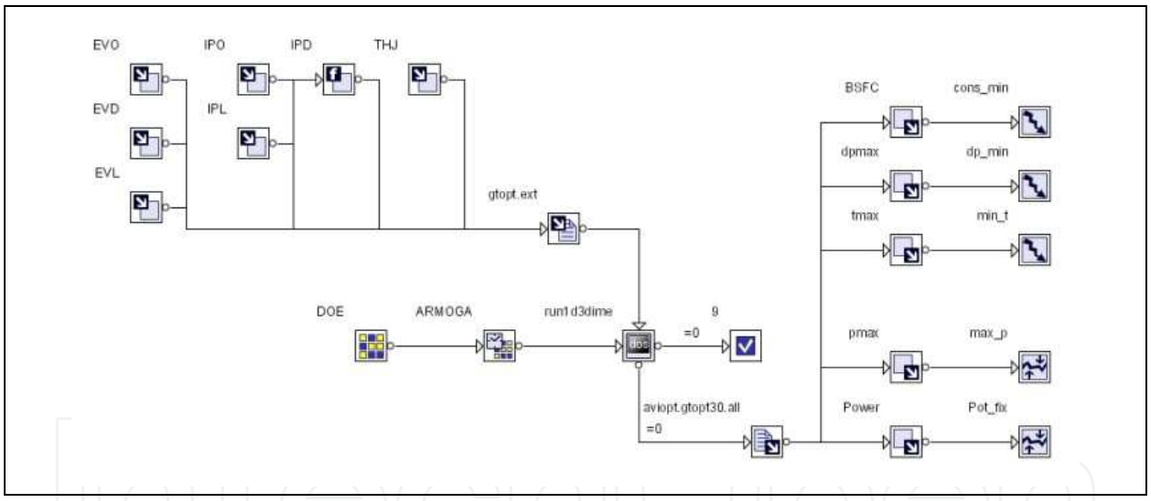


Fig. 14. Logic chart of the optimization procedure.

At each iteration, the values of the above variables are automatically written in the input file of the 1D code. ModeFrontier then runs the 1D code and extracts the required output results. After that, the independent variables are iteratively changed within prescribed intervals to the aim of finding the minimum fuel consumption. Additional objectives are also specified concerning the minimization of the pressure gradient and the minimization of the maximum average temperature inside the cylinder. In this way both noise and NOx emissions are expected to be reduced. Of course, each set of the independent variables must also guarantee the possibility to reach the prescribed power output (110 kW per bank) with a maximum pressure limited to 126 bar. These two additional requirements are fulfilled through the definition of two constraint variables in the logic scheme of figure 14.

Summarizing, a multi-objective constrained optimization problem is set-up, as follows:

Objective 1: min (BSFC)
Objective 2: min ($dp/dtheta_{max}$)
Objective 3: min ($T_{max}$)
Constrain 1: $p_{max}$ < 126 bar
Constrain 2: Power > 108 kW

To solve the above problem, the ARMOGA algorithm is utilized. The latter belongs to the category of genetic algorithms and employs a range adaptation technique to carry out time-consuming evaluations.
The specification of 3 objectives determines the existence of a two-dimensional Pareto frontier (Pareto surface) including all the solutions of the optimization problem.
Different sections of the Pareto surface are represented in figure 15 that highlights the presence of a clear trade-off between the three specified objectives. Due to the strong correlation between the maximum pressure and maximum temperature, a similar trade-off behaviour is found between the fuel consumption and the maximum pressure.
All the displayed points, however, respect the specified Constrain 1. The initial design point obtained in the previously discussed preliminary simulation, is located far away from the Pareto frontiers, as highlighted in the Figure 15. A relevant improvement of all the three objectives, hence, is surely realized.

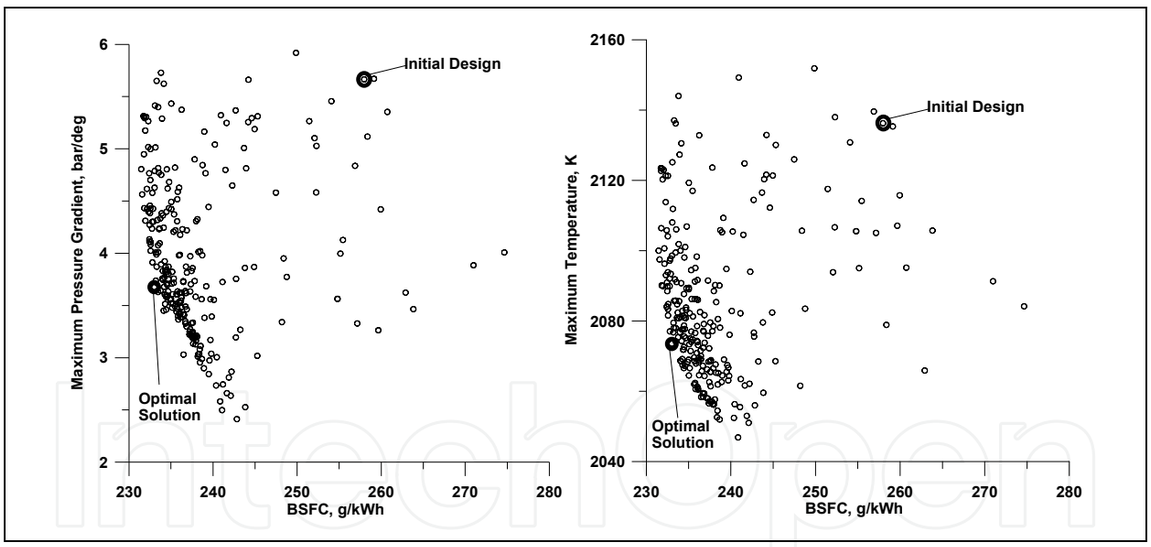


Fig. 15. Optimization results. Trade-off analysis.

In order to select a single solution among the ones located on the Pareto frontiers, the "Multi Criteria Decision Making" tool (MCDM) provided in modeFRONTIER™ is employed. It allows the definition of preferences expressed by the user through direct specification of attributes of importance (weights). BSFC and pressure gradient were considered as the most relevant parameters. Depending on the above relations, the MCDM tool is able to classify all the solution with a rank value. The solution which obtains the highest rank, therefore, can be identified. Basing on the described methodology, the solution with the highest rank value

is the one characterized by the identification number (ID) 238. The latter is also depicted along the Pareto frontiers in Figure 15.

| **Design ID** | **0** | **238** | **238-0** |
|---|---|---|---|
| **Input Variables** | **Value** | **Value** | **Delta** |
| EVO, deg ATDC | 80.00 | 94.17 | 14.17 |
| EVD, deg | 135.00 | 155.96 | 20.96 |
| EVL, mm | 12.00 | 14.66 | 2.66 |
| IPO, deg ATDC | 111.50 | 119.74 | 8.24 |
| THJ, deg ATDC | 347.49 | 351.69 | 4.2 |
| IPL, mm | 9.520 | 12.126 | 2.606 |
| **Transfer Variables** | **Value** | **Value** | **Delta** |
| IPD, deg | 137.00 | 120.53 | -16.47 |
| EVC, deg ATDC | 215.00 | 250.13 | 35.13 |
| IPC, deg ATDC | 248.50 | 240.27 | -8.23 |
| IPH, mm | 26.98 | 20.99 | -5.99 |
| **Objectives** | **Value** | **Value** | **% Var** |
| Min(BSFC), g/kWh | 257.98 | 233.01 | -9.68 % |
| Min(dP/dth), bar/deg | 5.665 | 3.676 | -35.11 % |
| Min(Tmax), K | 2136.3 | 2073.5 | -2.94 % |
| **Constraints** | **Value** | **Value** | **Delta** |
| Pmax < 126 bar | 125.83 | 97.43 | -28.4 |
| Power Output > 108 kW | 110.03 | 110.00 | ---- |

Table 1. Comparison between initial solution (ID=0) and "global optimum" (ID=238)

The position of the optimal solution also puts into evidence that the MCDM procedure effectively realizes a compromise between the conflicting needs, quantified by the attributes of importance described. In addition, this procedure defines a standardized method for the selection of the "global" optimum.

Table 1 reports a comparison between the initial and optimal solutions in terms of both independent (or input) variables, objectives parameters and constraints. Some other "transfer" variables, directly derived from the input data, are also listed.

The table puts into evidence that a BSFC improvement higher than 9% can be reached, together with a relevant reduction of both pressure gradient, maximum temperature and maximum pressure. This means that both a lower noise and NOx emission are expected, together with well lower thermal and mechanical stresses on the engine.

The above results are obtained thanks to a delayed opening of the exhaust valve and to an increased duration of exhaust phase. Contemporarily, a lower height and a greater width of the 14 intake ports are also selected by the optimization procedure.

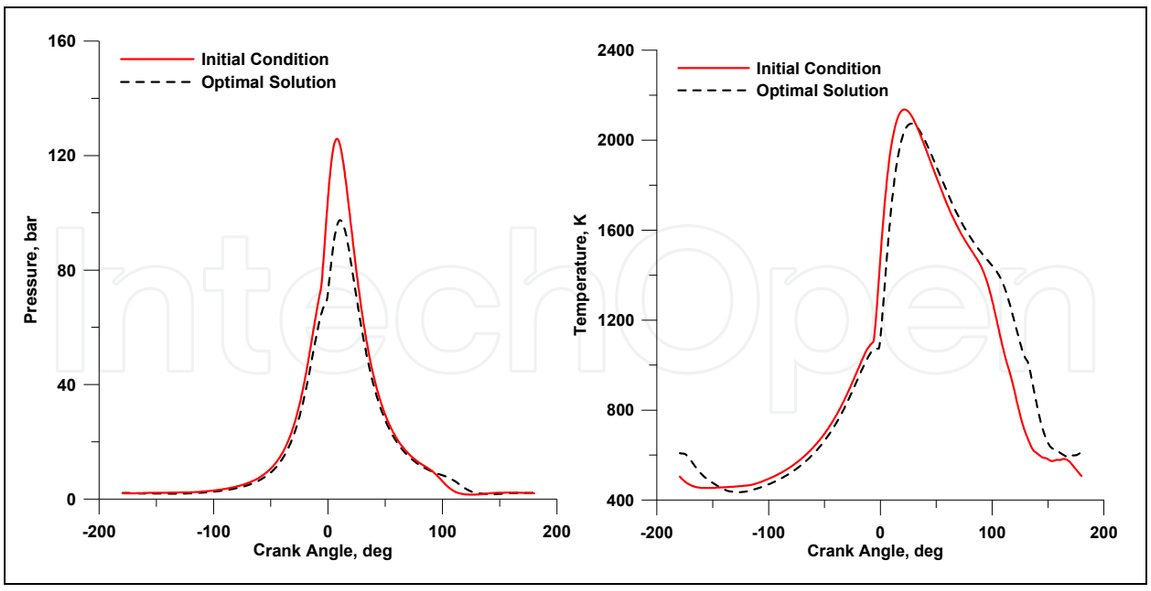


Fig. 16. Initial and optimal pressure and temperature cycles.

The delayed opening of the exhaust valve also produces an increased expansion work, as clearly observable in the in-cylinder pressure cycle plotted in Figure 16. The same figure highlights that a very lower pressure peak is obtained as a consequence of a lower supercharging level and a delayed injection start (see THJ variable in Table 1). Similar considerations can be draw looking at the average in-cylinder temperature profile.
Despite the lower boost pressure, the net shaft power remains the same, as requested by the Constrain 2, mainly due to a lower mechanical energy absorbed by the roots compressor.

It is worth putting into evidence that each modification to the engine geometry also determines a change in the operating conditions in terms of the super-charging level. This, together with a different power absorption of the roots, requires a control of the waste-gate opening in order to reach the prescribed power output at the engine shaft. In this sense, the optimization design regards the whole propulsion system, since it keeps into account the complex interaction between the various engine components.

## 4. Optimal selection of fuel injection strategies for a light-duty automotive engine

In this paragraph, a 3D modeling and an optimization procedure is applied to a naturally aspirated light-duty diesel engine (505 cm3 displacement). The engine is equipped with a mechanical Fuel Injection System (FIS) and is originally designed for non-road applications. Starting from the above base engine, a new prototype, equipped with a Common Rail (CR) FIS, is developed for being installed on small city-cars. The behavior of the CR injection system is firstly experimentally analyzed, in order to define the spray structure and injection rate realized under different operating conditions. As an example, in figure 17, the injection rates related to three different load conditions are compared. They are measured by an AVL Injection Gauge Rate System working on the Bosch tube principle. In addition, experimental

data on the spray tip penetration are available from the analysis of the liquid fuel spray images, carried out by image processing procedures (Alfuso et al., 1999; di Stasio et al., 1999). These data are employed to validate the spray model in the 3D CFD analysis (Allocca et al. 2004).

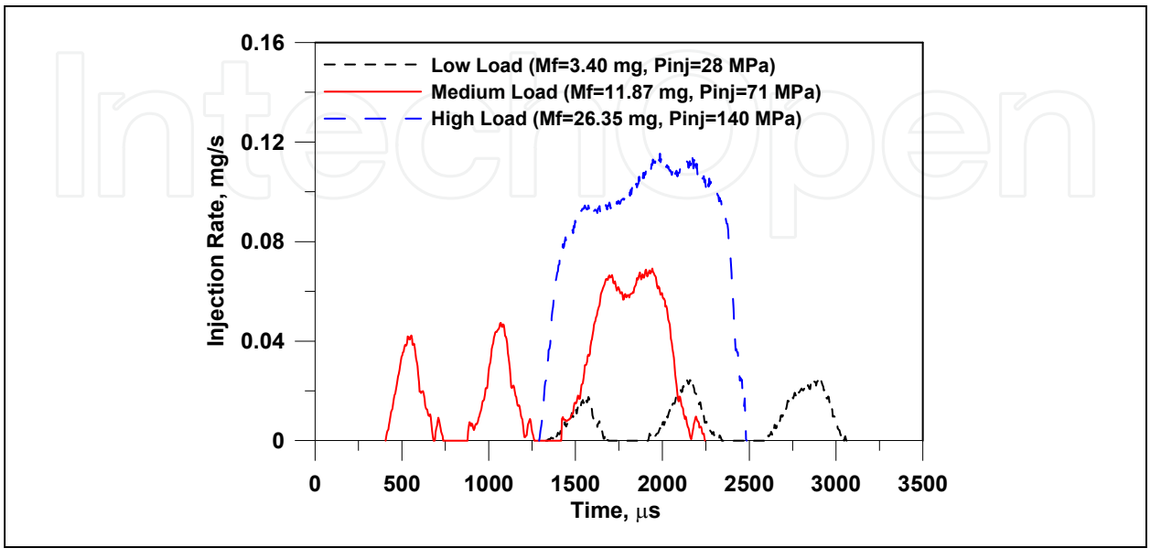


Fig. 17. Experimental injection rate of the CR-FIS.

Figure 18 summarizes the results of the preliminary numerical tuning of the spray break-up model, by comparing the experimentally measured penetration length and the numerical results. The Huh-Gosman and the Wave model are both tested and tuned by a change in the constants determining the aerodynamic break-up time, C2 and C1. Even with a value of 40 for the C2 constant, the Huh-Gosman model underestimates the spray penetration length, whereas quite reliable results are achieved by activating the Wave model with C1=60.

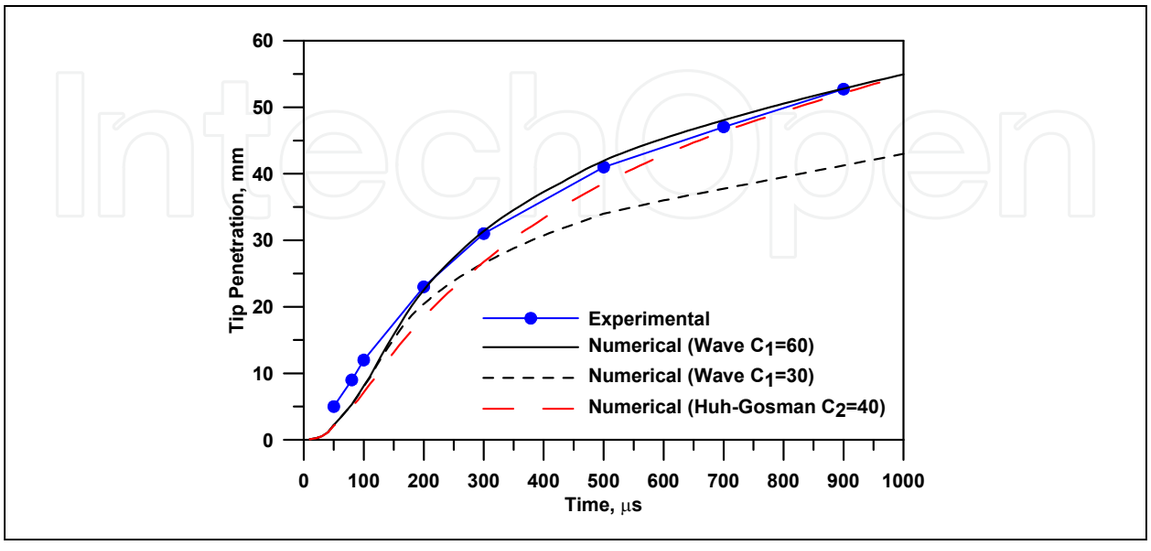


Fig. 18. Numerical and experimental spray penetration length.

The tuned spray model is part of a more complete 3D CFD analysis. Figure 19 shows a top view of the unstructured grids employed in the calculations.

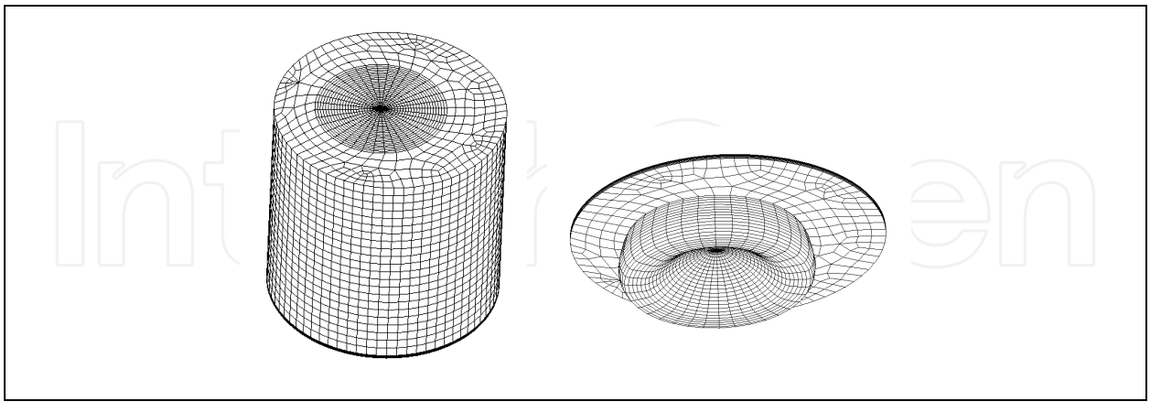

Fig. 19. A top view of the grid at the BDC, and a bottom view of the grid at the TDC

During the 3D analysis, a three pulses injection strategy is specified as shown in Figure 20, compared to the actual experimental profile. Five degrees of freedom – namely the start of pilot injection (soip), the dwell time between the first and second pulse (dwell_1), the dwell time between the second and third pulse (dwell_2), and the percentages of fuel mass injected during the first two pulses – completely define the overall injection profile.

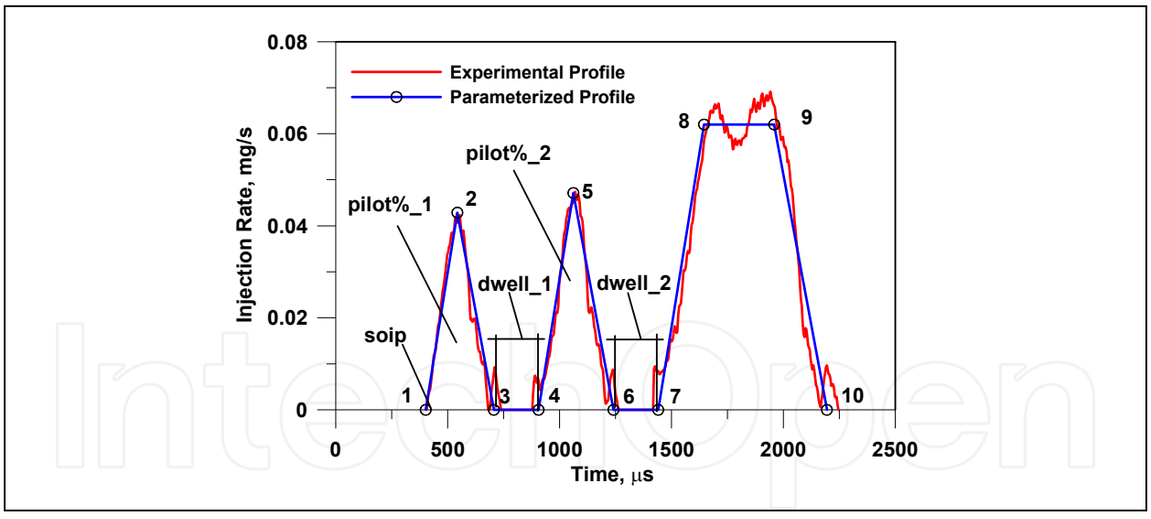


Fig. 20. Parametric Injection strategy at medium load

In this way, by varying the above 5 parameters, different combustion developments and noxious emissions arises. Each predicted pressure cycle is also processed to estimate the combustion-radiated noise, with the simplified approach previously described.
The optimization problem is settled in order to identify the 5 control parameters with the aim of simultaneously minimizing fuel consumption, pollutant emissions and radiated noise. The logical development of the optimization problem within the ModeFRONTIER™ environment is explained in figure 21.

Figure 22 displays the scatter charts of the 440 points computed along the optimization process, highlighting the complex interactions among the various objectives. A clear trend exists between the IMEP and the Overall Noise. A greater dispersion of the results is found looking at the trade-off between NO and soot mass fractions.

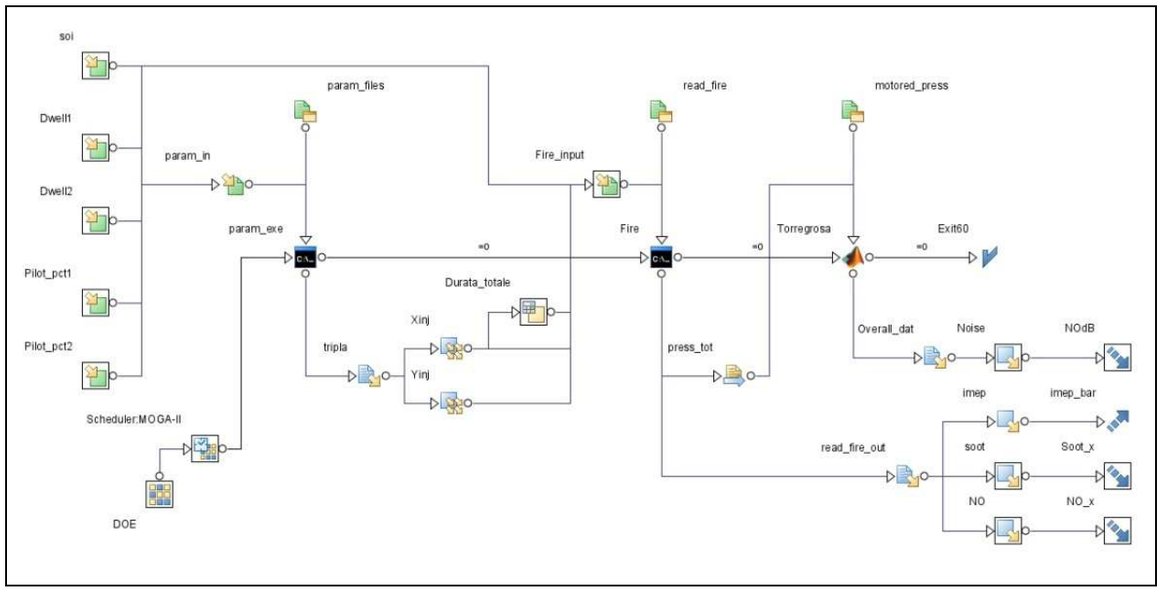


Fig. 21. Logic scheme of the optimization process within ModeFRONTIER

The "Multi Criteria Decision Making" tool (MCDM) provided in modeFRONTIER™ is finally employed to select single solutions among the ones reported in figure 22.

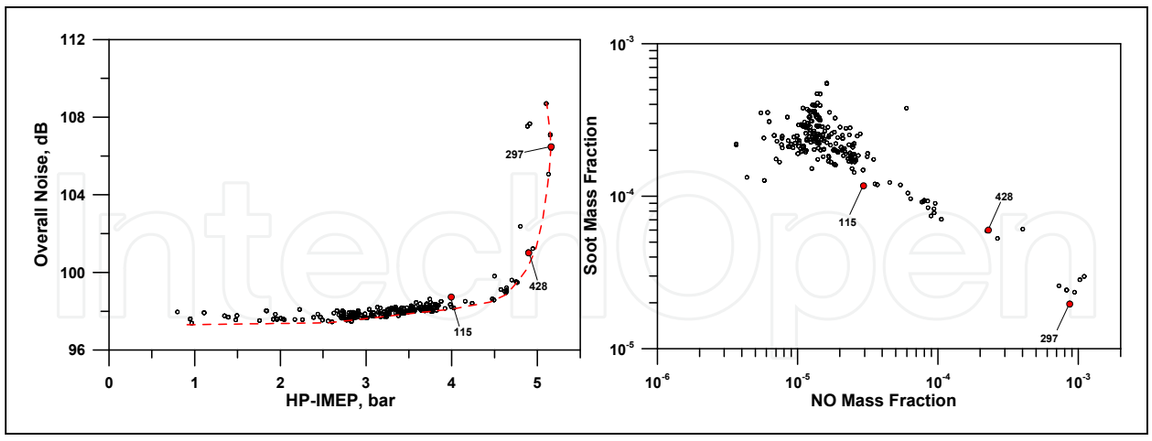


Fig. 22. Scatter charts of the optimization process

Three different solutions are identified, the first one selecting the IMEP and soot as the most important parameters (solutions #297). In the second and third one, the importance of NO emission and Overall Noise are more and more increased (solutions #428 and #115, respectively).

Figure 23 compares the related optimal injection strategies, while figure 24 finally shows the pressure cycles, the heat release rates, and the NO and soot production. High IMEP and low soot are obtained with a very advanced start of both pilot and main injections (solutions #297). This strategy determines the highest pressure peak and IMEP, while at the same time producing the highest heat release peak and pressure gradient, responsible of increased NO amounts and Noise level. Although introducing some IMEP and soot penalization, a radically lower Noise level and a better NO emission is found with a delayed soip and smaller dwell times (solution #428).

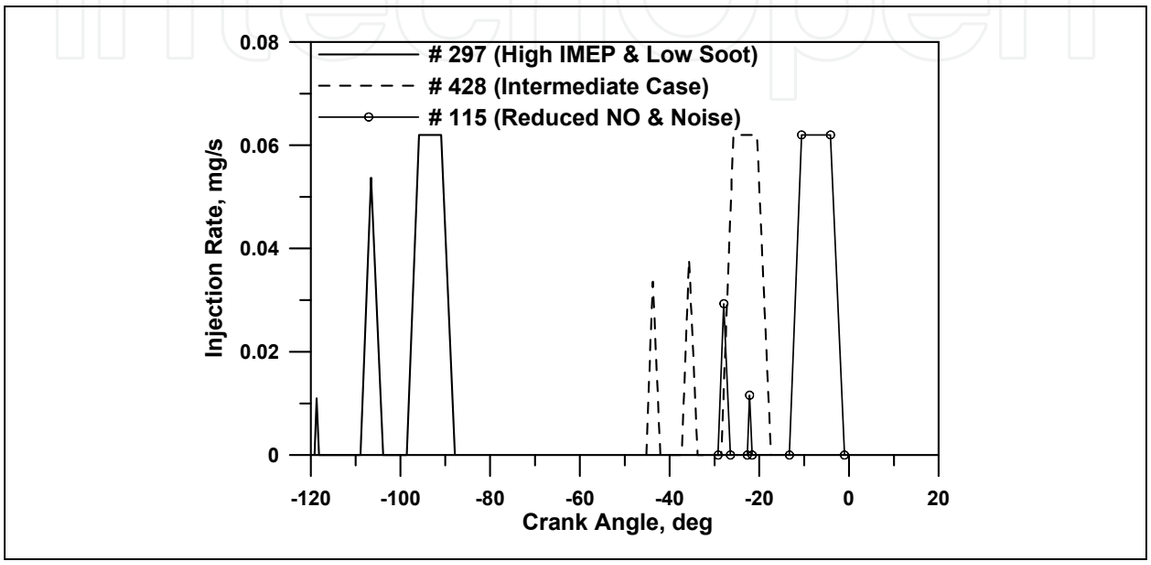


Fig. 23. Optimal injection strategies

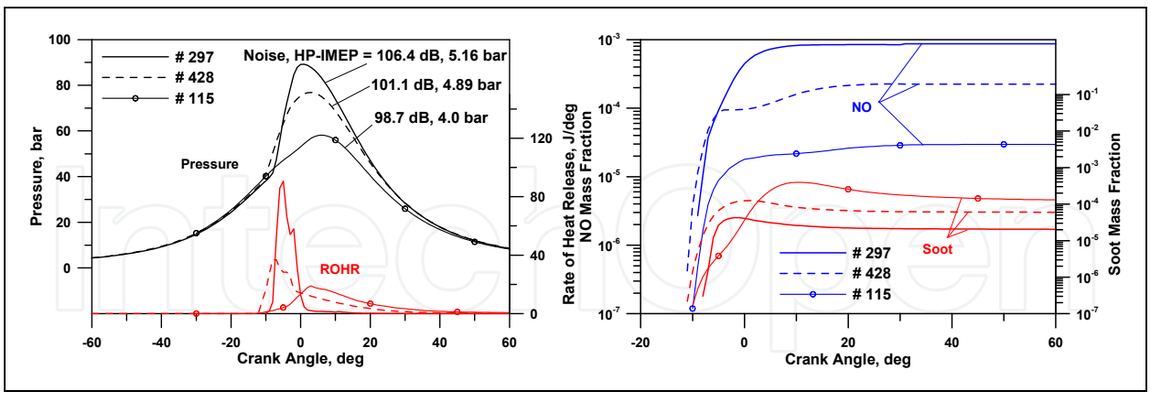


Fig. 24. Comparisons of the pressure cycles, heat release, NO and soot emission

In this case a very smoother heat release is found (fig. 24). The main path for a substantial noise reduction is indeed the specification of a much delayed pilot and a still more delayed main injection (solution #115). Both these effects, in fact, contribute in reducing the heat release rate and the pressure gradient during the combustion process, even if a non-negligible mechanical output loss has to be expected. This last strategy probably represents the best compromise solution in terms of pollutant species production and radiated noise.

However, being the present results obtained at a constant overall injected fuel mass, the lower power output obtained in this case directly impacts on the specific fuel consumption and on the CO2 emission. This demonstrates the difficulties in identifying an optimal injection strategy, able to complying with so many conflicting needs, even when a highly modulated injection process is considered.
As a conclusive remark, the optimization procedure is able to capture the expected effects of the injection parameters on the overall performance and radiated noise and provides a method for the choice the best compromise solution. The methodology can be easily extended to multiple operating conditions and can include additional variables (injection pressure, swirl ratio, boost pressure, EGR rate) and objectives (CO and HC production). In this way a variable combustion mode, like standard premixed-diffusive, HCCI (Bression et al, 2008; Zavala et al. 2001), PLTC (Shimazaki et al. 2003; Kalghatgi, 20009), etc. can be realized, depending on operating conditions and selected objectives.

## 5. Conclusion

The present chapter presented two different examples for the design and analysis of modern CR equipped Diesel engines. A tool for multi-objective optimization was found very useful at the engine design stage to reduce the time-to-market of new engine prototypes, thanks to the possibility to effectively evaluate the influence of geometrical and operating engine parameters. In addition, a similar technique was applied to find the optimal selection of the control parameters (namely the injection strategy) in order to obtain an better engine behaviour. To reach the above objectives, different simulation techniques were employed, resorting to 1D, 3D and acoustic analyses. More accurate or simplified approaches were presented and differently used along the different phases of the engine development process. In each case, a continuous exchange of information among the various methods allowed to improve the overall simulation accuracy and results reliability. The whole procedure hence represents a very useful tool to reduce the huge experimental activity usually required to design and develop a modern CR diesel engine.

## 6. References

Alfuso, S., Allocca, L., Corcione, F.E., di Stasio S. (1999) “Image Diagnostics of Common Rail Diesel Sprays Evolving in Nytrogen Ambient at Different Densities”, ICE’99 Internal Combustion Engines: Experiments and Modeling.

Alfuso, S., Allocca, L., Auriemma, M., Caputo, G., Corcione, F.E., Montanaro, A., Valentino, G. (2005) “Analysis of a High Pressure Diesel Spray at High Pressure and Temperature Environment Conditions”, SAE Paper 2005-01-1239

Allocca, L., Corcione, F.E., Costa, M. (2004) “Numerical and Experimental Analysis of Multiple Injection Diesel Sprays”, SAE Paper 2004-01-1879

Bression, G., Soleri, D., Dehoux, S., Azoulay, D., Hamouda, H., Doradoux, L., Guerrassi, N. Lawrence, N.J. (2008) “A Study of Methods to Lower HC and CO Emissions in Diesel HCCI”, SAE Paper 2008-01-0034

Colin, O., and Benkenida, A. (2004) "The 3-Zones Extended Coherent Flame Model (ECFM3Z) for Computing Premixed/Diffusion Combustion", Oil & Gas Science and Technology, IFP, Vol. 59, N. 6, pp. 593-609

Costa, M., Siano, D., Valentino, G., Corcione, F.E., Bozza, F. (2009) "Prediction and Optimization of the Performances, Noxious Emissions and Radiated Noise of a Light Duty Common-Rail Diesel Engine", proceedings of 9th International Conference on Engines and Vehicles (ICE2009)

di Stasio, S., Alfuso, S., Allocca, L., Corcione, F.E. (1999) "Experimental Study on the Atomization Mechanism for Fuel Sprays Evolving in Atmospheres of Different Nature and Density" - ImechE Seminar Publication 1, 17, pp.241-255

Dukowicz, J.K. (1980) "A Particle-Fluid Numerical Model for Liquid Sprays", J. Comp. Physics, 35, 229-253

Kalghatgi, G. (2009) "Is Gasoline the Best Fuel for Advanced Diesel Engines? – Fuel Effects in "Premixed-Enough" compression ignition Engines", Towards Clean Diesel Engines, TCDE2009

Liu, A.B. and Reitz, R.D. (1993) "Modeling the Effects of Drop Drag and Break-up on Fuel Sprays", SAE 930072

O'Rourke, P.J. (1989) "Statistical Properties and Numerical Implementation of a Model for Droplet Dispersion in Turbulent Gas", J. Comput. Physics 83

Papalambros, P.V., and Wilde, D.J.(2000) "Principles of Optimal Design Modeling and Computation", Cambribde University Press, Cambridge

Payri, F., Broatch, A., Tormos, B., Marant, V., (2005) "New methodology for in-cylinder pressure analysis in direct injection diesel engines—application to combustion noise", Meas. Sci. Technol. 16 540–547 doi:10.1088/0957-0233/16/2/029

Sasaki, D. (2005) "ARMOGA, An efficient Multi-Objective Genetic Algorithm", Technical Report

Shimazaki, N., Tsurushima, T., Nishimura, T. (2003) "Dual Mode Combustion Concept with Premixed Diesel Combustion by Direct Injection Near Top Dead Center", SAE 2003-01-0742

Siano, D., Bozza, F., Costa, M. (2008) "Optimal Design of a Two-Stroke Diesel Engine for Aeronautical Applications Concerning both Thermofluidynamic and Acoustic Issues", IMECE2008-68713, Proceedings of 2008 ASME International Mechanical Engineering Congress and Exposition, Boston, Massachusetts, USA.

Stephenson, P.W. (2008) "Multi-Objective Optimization of a Charge Air Cooler using modeFRONTIER and Computational Fluid Dynamics", SAE Paper 2008-01-0886

Stotz, M., Schommers, J., Duvinage, F., Petrs, A., Ellwanger, S., Koynagi, K., Gildein, H. (2000) "Potential of Common-Rail Injection System for Passenger Car Di Diesel Engines", SAE Paper 2000-01-0944

Torregrosa, A.J., Broatch, A., Martın J., Monelletta, L. (2007) "Combustion noise level assessment in direct injection Diesel engines by means of in-cylinder pressure components", Meas. Sci. Technol., 18 2131-2142, doi:10.1088/0957-0233/18/7/045,

Zavala, P.A.G., Pinto, M.G, Pavanello, R., Vaqueiro J. (2001) "Comprehensive Combustion Noise Optimization", Sae Paper 2001-01-1509


**Fuel Injection**

Edited by Daniela Siano

ISBN 978-953-307-116-9
Hard cover, 254 pages
**Publisher** Sciyo
**Published online** 17, August, 2010
**Published in print edition** August, 2010

Fuel Injection is a key process characterizing the combustion development within Internal Combustion Engines (ICEs) and in many other industrial applications. State of the art in the research and development of modern fuel injection systems are presented in this book. It consists of 12 chapters focused on both numerical and experimental techniques, allowing its proper design and optimization.



INTECH
open science | open minds

**InTech Europe**
University Campus STeP Ri
Slavka Krautzeka 83/A
51000 Rijeka, Croatia
Phone: +385 (51) 770 447
Fax: +385 (51) 686 166
www.intechopen.com

**InTech China**
Unit 405, Office Block, Hotel Equatorial Shanghai
No.65, Yan An Road (West), Shanghai, 200040, China
中国上海市延安西路65号上海国际贵都大饭店办公楼405单元
Phone: +86-21-62489820
Fax: +86-21-62489821

IntechOpen